Transients in the Oxidative and H-Atom-Induced Degradation of 1,3,5-Trithiane. Time-Resolved Studies in Aqueous Solution

5 AUTHORS, INCLUDING:

Klaus-Dieter Asmus
Adam Mickiewicz University
89 PUBLICATIONS   3,162 CITATIONS

SEE PROFILE

Lily Hug
University of Greenwich
114 PUBLICATIONS   2,658 CITATIONS

SEE PROFILE

Krzysztof Bobrowski
Instytut Chemii i Techniki Jądrowej
129 PUBLICATIONS   2,042 CITATIONS

SEE PROFILE

Transients in the Oxidative and H-Atom-Induced Degradation of 1,3,5-Trithiane. Time-Resolved Studies in Aqueous Solution

Klaus-Dieter Asmus,[†] Gordon L. Hug,[†,‡,#] Krzysztof Bobrowski,[§] Quinto G. Mulazzani,[‖] and Bronislaw Marciniak*,[†]

Faculty of Chemistry, Adam Mickiewicz University, 60-780 Poznan, Poland, Radiation Laboratory, University of Notre Dame, Notre Dame, Indiana 46556, Institute of Nuclear Chemistry and Technology, 03-195 Warsaw, Poland, and ISOF, Consiglio Nazionale delle Ricerche, 40129 Bologna, Italy

The $^{\bullet}$OH-induced oxidation of 1,3,5-trithiacyclohexane (**1**) in aqueous solution was studied by means of pulse radiolysis with optical and conductivity detection. This oxidation leads, via a short-lived $^{\bullet}$OH radical adduct (<1 μs), to the radical cation $\mathbf{1}^{\bullet+}$ showing a broad absorption with λ_{max} equal to 610 nm. A defined pathway of the decay of $\mathbf{1}^{\bullet+}$ is proton elimination. It occurs with $k = (2.2 \pm 0.2) \times 10^4$ s^{-1} and yields the cyclic C-centered radical $\mathbf{1}(-\text{H})^{\bullet}$. The latter radical decays via ring opening (β-scission) with an estimated rate constant of about 10^5 s^{-1}. A distinct, immediate product (formed with the same rate constant) is characterized by a narrow absorption band with $\lambda_{max} = 310$ nm and is attributed to the presence of a dithioester function. The formation of the 310 nm absorption can be suppressed in the presence of oxygen, the rationale for this being a reaction of the C-centered cyclic radical $\mathbf{1}(-\text{H})^{\bullet}$ with O$_2$. The disappearance of the 310 nm band (with a rate constant of 900 s^{-1}) is associated with the hydrolysis of the dithioester functionality. A further aspect of this study deals with the reaction of H$^{\bullet}$ atoms with **1** which yields a strongly absorbing, three-electron-bonded $2\sigma/1\sigma^*$ radical cation $[\mathbf{1}(\text{S}\therefore\text{S})-\text{H}]^+$ ($\lambda_{max} = 400$ nm). Its formation is based on an addition of H$^{\bullet}$ to one of the sulfur atoms, followed by β-scission, intramolecular sulfur−sulfur coupling (constituting a ring contraction), and further stabilization of the S$\therefore$S bond thus formed by protonation. $[\mathbf{1}(\text{S}\therefore\text{S})-\text{H}]^+$ decays with a first-order rate constant of about 10^4 s^{-1}. Its formation can be suppressed by the addition of oxygen which scavenges the H$^{\bullet}$ atoms prior to their reaction with **1**. Complementary time-resolved conductivity experiments have provided information on the quantification of the $\mathbf{1}^{\bullet+}$ radical cation yield, the cationic longer-lived follow-up species, extinction coefficients, and kinetics concerning deprotonation processes as well as further reaction steps after hydrolysis of the transient dithioesters. The results are also discussed in the light of previous photochemical studies.

Introduction

The presence of multiple sulfur functionalities renders 1,3,5-trithiane a most interesting compound with respect to redox chemistry. It is well established that a one-electron oxidation of an organic sulfide primarily leads to a sulfur-centered radical cation, R$_2$S$^{\bullet+}$, which stabilizes either by resonance (e.g., if R = Aryl) or interaction with a free electron pair provided by a second sulfur atom (typically in case of nonaromatic sulfides).[1−5] The latter yields, as a result of p orbital overlap, a $2\sigma/1\sigma^*$ three-electron bond between the two sulfur atoms, >S$\therefore$S<, in which two electrons form a normal σ bond while the third electron accommodates itself in an antibonding, i.e., bond-weakening orbital. This stabilization occurs *inter-* as well as *intra*molecularly with the former depending on the sulfide concentration, while the intramolecular process requires, in particular, a geometry of the two interacting p orbitals which is favorable for overlap. The underlying concept has been verified in numerous experimental examples (mostly, but not exclusively,

in aqueous systems)[1−4,6−9] and underpinned by convincing theoretical calculations.[10−13] Furthermore, this kind of bonding is not restricted to sulfur-containing compounds but may involve any other electronically suitable atoms. Especially good candidates, besides S, in this respect are the other higher (heavier) atoms in groups V−VII of the periodic table, that is, P, Se, Te, Cl, Br, and I.[14−18] Reasonably stable three-electron bonds have, however, also been observed involving N and O when these heteroatoms constituted part of sterically rigid, typically five- or six-membered ring structures.[18−24]

A characteristic feature of these three-electron bonded species is an optical, typically broad, absorption which, depending on structure and substitution, exhibits a maximum anywhere between the near UV and near-infrared. Typically, the better the p orbital overlap is and the stronger the two-center three-electron (2c−3e) bond is, the more blue-shifted and narrower the absorption band is. Substitution by electron-density releasing groups at sulfur, on the other hand, results in a red shift. Extreme experimental examples in sulfur-containing systems are (H$_2$S$\therefore$SH$_2$)$^+$ ($\lambda_{max} = 380$ nm)[25,26] and (Me,*t*-BuS$\therefore$S*t*-Bu$_2$)$^+$ ($\lambda_{max} = 600$ nm)[27,28] for intermolecular, and $\mathbf{2}^{\bullet+}$ ($\lambda_{max} = 400$ nm)[7] and $\mathbf{3}^{\bullet+}$ ($\lambda_{max} = 650$ nm)[29] (see Chart 1) for intramolecular systems, respectively. Spectroscopically, the absorption is, in first approximation, due to a $(\sigma-\text{n}) \rightarrow \sigma^*$ transition where n

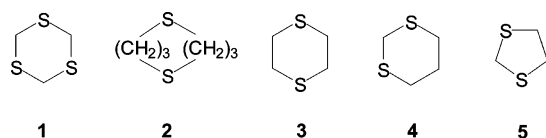* E-mail: marcinia@amu.edu.pl.
† Adam Mickiewicz University.
‡ University of Notre Dame.
# Fulbright Scholar, Faculty of Chemistry, AMU. Permanent address: Radiation Laboratory, UND.
§ Institute of Nuclear Chemistry and Technology.
‖ ISOF.

Transients in the Degradation of 1,3,5-Trithiane

J. Phys. Chem. A, Vol. 110, No. 29, 2006 **9293**

CHART 1: List of Compounds

reflects the combined electronic contributions of the rest-molecule besides sulfur.

An interesting extension occurs for molecules containing more than two, not directly connected, sulfur atoms in the same molecule, the simplest example being 1,3,5-trithiane, **1**. The one-electron oxidation product, namely, the **1**[•+] radical cation shows an absorption with λ_{max} equal to 610 nm.[30] With respect to the position of the maximum, it does not differ very much from the radical cation derived from 1,3-dithiane **4**[•+] ($\lambda_{max} = 600$ nm).[30] This has been explained by photoelectron spectroscopy data[31,32] which indicate that the sulfur–sulfur interaction in **1**[•+] involves mainly just two S atoms, that is, closely resembles the situation in **4**[•+]. The third sulfur in **1**[•+], nevertheless, participates electronically which shows up in a significant broadening of the absorption band of **1**[•+] as compared to that of **4**[•+]. Such multicentered radical cations have also been observed as transients in the one-electron oxidation of **1** in nonaqueous, aprotic solvents.[30,33] In this kind of environment, even dimer radical cation complexes $(1)_2$[•+] can be stabilized with an apparent delocalization of charge and spin over up to six sulfur atoms and with very red-shifted absorptions ($\lambda_{max} = 750$ nm).[30,33]

Another most characteristic feature in the oxidation of **1** is the formation of a species which results from the decay of **1**[•+] and which exhibits a relatively long-lived, strong but rather narrow band with λ_{max} at 310 nm (half-width $\approx$ 50 nm). As will be shown in this paper, these species are neutral radicals. The same kind of absorption band with respect to origin, λ_{max} and width has also been observed in the oxidation of **4** and other 1,3-dithia compounds such as **5**.[34] On the other hand, no such absorption band is generated in the oxidation of **3**. The 1,3-dithia configuration thus appears to be an essential prerequisite for the formation of the species absorbing around 310 nm.

A most interesting finding in this context is provided by steady-state photolysis studies conducted with **1** (and methyl and aryl derivatives thereof) in acetonitrile solutions.[35,36] Product analysis, in particular, has revealed the formation of several stable compounds which show practically the same absorption characteristics, that is, with λ_{max} at about 310 nm, as the transient radicals mentioned above. The question arising in this context is, therefore, how these stable oxidation products relate to the transient species observed in time-resolved studies. Further experimental results and interpretations, reported in this paper, will reveal that the absorbing chromophore in both the transient radicals and nonradical stable products is a thioester moiety.

Our study includes experiments at various pHs. In doing this, it was noticed that in very acidic solution of **1** a new transient species was formed which appeared to be generated via a reaction of hydrogen atoms with a sulfur atom in **1**. This is interesting since the sulfur atom in thioethers is usually not the primary target of H[•], despite some, mostly recent,[37–40] reports. H atoms rather tend to abstract hydrogen atoms from C–H bonds, particularly if these are activated by neighboring functionalities such as sulfur atoms. In this part of our present study, we will identify and characterize this new species as a $2\sigma/1\sigma*$ three-electron bonded, sulfur-centered radical cation.

Experimental Section

All solutions investigated were aqueous ones with the solvent being deionized, Millipore-filtered H_2O, the quality of which corresponded to triply distilled water. 1,3,5-Trithiane, **1**, was added to achieve a saturated (ca. 10^{-4} M) solution. Treatment of the solution by ultrasound assisted this process although usually a small amount of **1** remained undissolved. Experiments were always conducted with the clear part of the solution. Variations of pH were achieved by appropriate additions of $HClO_4$ or NaOH. Other chemicals, including all sulfur compounds were of the purest grade available.

The investigation of transients was performed by means of pulse radiolysis, with both optical and conductivity detection. The actual experiments have been conducted with the pulse radiolysis equipments at the CNR facilities at Bologna (Italy), the Institute for Nuclear Chemistry & Technology at Warsaw (Poland), and the Radiation Laboratory at the University of Notre Dame. All these facilities and the above-mentioned detection techniques have been described in detail previously.[41–44] Analysis of absorption–time and conductivity-time traces was generally based on signal sampling and averaging over an appropriate number of pulses. Dosimetry and calibration of optical and conductivity measurements were based on thiocyanate and dimethyl sulfoxide systems, respectively. Typical pulses used were of 5–50 ns duration and generated radical concentrations in the 10^{-6}–10^{-5} M range. Details for the evaluation of optical and conductivity data have been published elsewhere.[45–48]

Oxidations were generally initiated by hydroxyl radicals which, besides hydrated electrons and hydrogen atoms, are primary radical species generated upon the radiolysis of water. In neutral solutions, the yields of [•]OH and e_{aq}^- amount to 0.28 μmol J[−1] each, while H[•] are formed with 0.06 μmol J[−1]. For the study of hydroxyl radical reactions, solutions were saturated with N_2O. This converts hydrated electrons according to $N_2O + e_{aq}^- + H_2O \rightarrow {}^•OH + N_2 + OH^-$, that is, practically doubles the available [•]OH yield. For the investigation of hydrogen atom reactions, solutions were acidified so that all hydrated electrons were converted according to $H^+ + e_{aq}^- \rightarrow H^•$.

All experiments were carried out at ambient temperature, generally 18–22 °C. Error limits of individual pulse radiolysis experiments remained within the generally accepted limit of ±10%. Deviations from this value in either direction are explicitly noted.

Results and Discussion

Optical Pulse Radiolysis Experiments. *Transient Spectra.* Saturated aqueous solutions of **1** were investigated with respect to the formation and decay of transients. At all pHs, covering a range between 4 and 10.5, the initial absorption spectrum detectable on the ns to lower μs time scale showed a broad band with a distinct maximum at 610 nm, small bands at around 340 and 400 nm, and some less defined absorptions below 300 nm toward the UV. The entire transient spectra recorded at about 150 ns, 3 μs, and 150 μs after the 5 ns pulse are shown in Figure 1.

The earliest, reasonably distinct, although small band is that observable at 340 nm at 150 ns. It resembles that of typical [•]OH adducts to sulfur formed as primary transients in several [•]OH-induced oxidations of, for example, aliphatic sulfides and 1,4-dithiacyclohexane (**3**).[6,29,49,50] This band is very short-lived; at the later recording time of 3 μs, it is not as distinct anymore and may, in fact, have disappeared already. Structurally, this species may best be viewed as a sulfuranyl-type radical
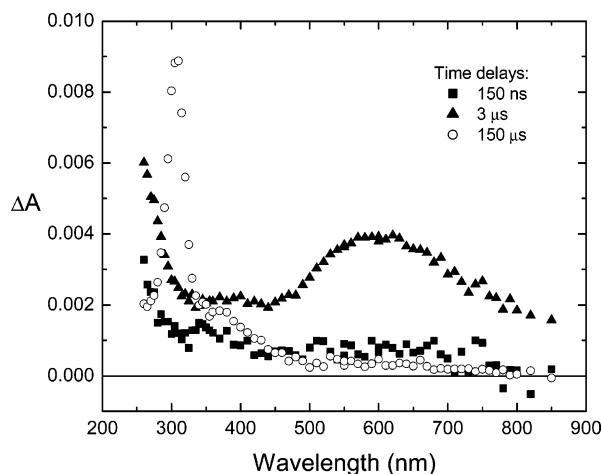
Figure 1. Transient absorption spectra recorded after radiolysis of **1** in N_2O-saturated aqueous, pH 9.3 solutions ([**1**] ca. 10^{-4} M) at various time delays after the pulse.

SCHEME 1
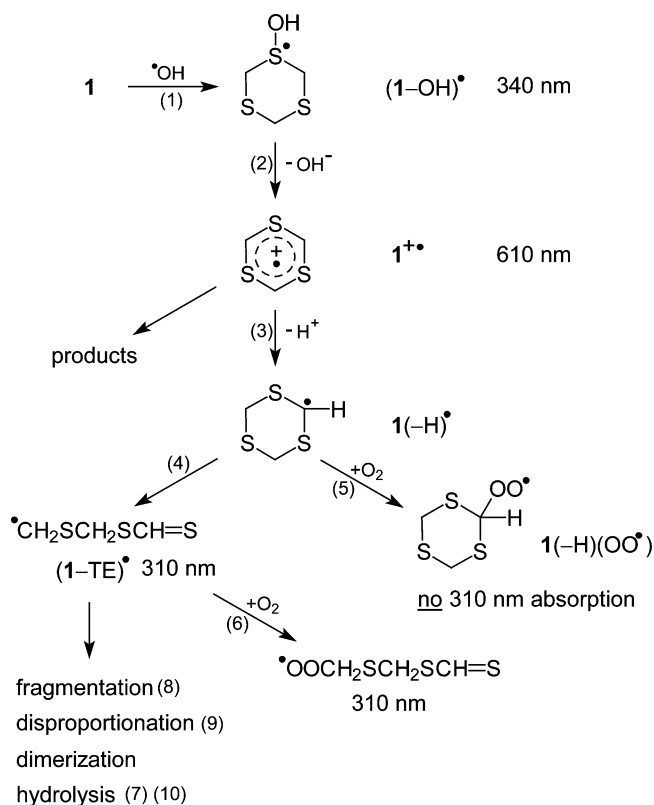
(**1**−OH)$^•$ (Scheme 1) owing to the significant difference in electronegativity between sulfur and oxygen. Depending on pH the −S$^•$−OH group may also deprotonate, yielding the −S$^•$−O$^-$ radical anion. The latter have been identified, for example, in the one-electron reduction of sulfoxides.[51] Our present data concerning the $^•$OH reaction with **1** do not, however, allow any further conclusions in this direction.

After the first few μs the 610 nm band is fully developed. It practically exhibits the same features as the 610 nm transient reported in an earlier study of ours.[30] Accordingly, this band is attributed to the intramolecular radical cation **1**$^{•+}$. With the decay of this species a strong and narrow 310 nm band emerges. This process is practically completed after about 150 μs. The 310 nm absorption is relatively long-lived and eventually decays in the millisecond time domain. The other apparent, although small band at around 400 nm seems to be formed about as fast as the
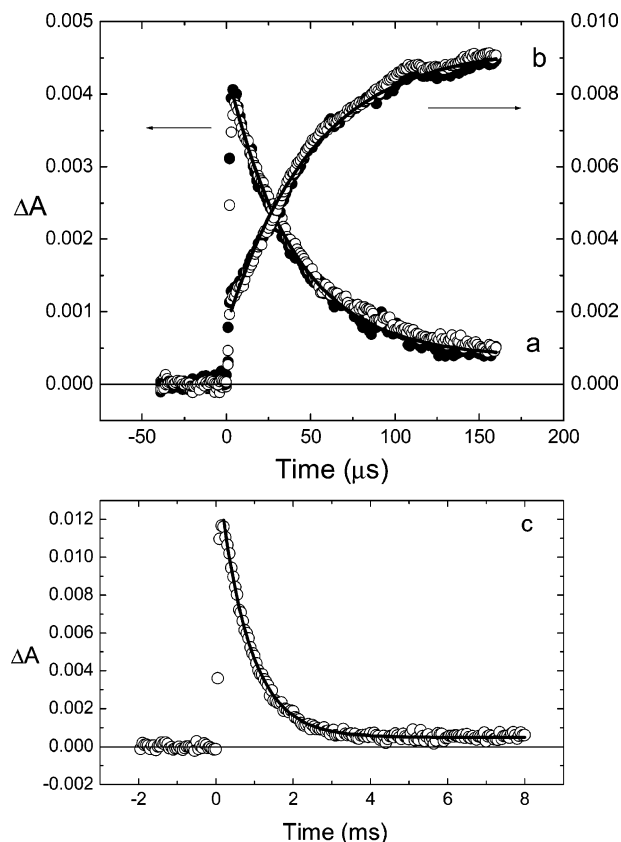
Figure 2. (a) Absorption−time traces recorded at 610 nm on the microsecond time-scale following pulse irradiation of **1** in N_2O-saturated aqueous solutions ([**1**] ca. 10^{-4} M) at pH 4 (open circles) and pH 9 (filled circles); (b) absorption−time traces of the same two solutions and under the same conditions as in panel a but recorded at 310 nm (open circles pH 4, filled circles pH 9); (c) absorption−time traces recorded at 310 nm on the millisecond time scale following pulse irradiation of **1** in N_2O-saturated aqueous solutions ([**1**] ca. 10^{-4} M) at pH 10.

610 nm band but exhibits a much longer lifetime than the latter, indicating that the 400 nm and 610 nm species are of different nature. As will be discussed later, the first three species ((**1**−OH)$^•$, **1**$^{•+}$, (**1**−TE)$^•$) are directly linked to each other in the $^•$OH-induced reaction sequence displayed in Scheme 1. The 400 nm species, on the other hand, results from the reaction of **1** with H$^•$ atoms, with the underlying mechanism for this process being shown in Scheme 2 (vida infra).

Kinetics. The formation of the 340 nm $^•$OH adduct, (**1**−OH)$^•$, via reaction 1 could not be time-resolved with desirable accuracy because of its very short lifetime and the uncertainty in the concentration of **1**. A diffusion-controlled process with $k_1 \approx (5-10) \times 10^9$ M^{-1} s^{-1} would, however, be in reasonable accord with the experimental observation.

The decay of (**1**−OH)$^•$ into the radical cation **1**$^{•+}$ (reaction 2) was kinetically resolved by analyzing the formation of the 610 nm absorption. The process was of first order and occurred with $k_2 = (1.2 \pm 0.1) \times 10^6$ s^{-1}, irrespective of pH (within pH 4.0−10.4 range).

Practically no effect of pH has also been observed with respect to the yield and decay of **1**$^{•+}$. Figure 2a exhibits, for example, absorption−time traces at 610 nm, recorded by pulse irradiating solutions at pH 4 and 9. A first-order rate constant of $k_3 = (2.2 \pm 0.2) \times 10^4$ s^{-1} was derived from a reasonably satisfactory computer-aided fit of an exponential. It is assigned to the proton loss from **1**$^{•+}$, a process unambiguously corroborated by time-resolved conductivity measurements (vide

Transients in the Degradation of 1,3,5-Trithiane

J. Phys. Chem. A, Vol. 110, No. 29, 2006 **9295**

infra). As will be concluded from further experiments in the presence of oxygen (vide infra), the immediate result of this process is the cyclic, C-centered 2-yl radical $1(-H)^\bullet$.

Close inspection of both decay curves reveals that the decay at, for example, 610 nm does not, however, seem to lead completely back to the original baseline at longer times. A possible reason could be some minor second-order contribution to the decay of $1^{\bullet+}$ which is, in fact, indicated in some high dose experiments. Raising the dose from 8.4 to 51.0 Gy, that is, the concentration of $1^{\bullet+}$ from 0.5×10^{-5} to 3×10^{-5} M (in pH 10 solutions), the first half-lives of the 600 nm absorption dropped slightly by a factor of 2. A small contribution of a second-order decay of $1^{\bullet+}$ is further corroborated by the results of time-resolved conductivity experiments (vide infra).

Simultaneous recordings at 310 nm revealed the formation of a longer-lived species. The relevant traces, recorded on the same microsecond time scale as the 610 nm traces, are shown in Figure 2b. The first-order rate constants, derived from exponential rate fittings for the formation of this absorption, are $(2.2 \pm 0.4) \times 10^4$ s^{-1}; that is, they are identical with those for the decay of the absorption at 610 nm. Furthermore, they also remain the same over the investigated pH 4–10 range.

What is the identity of the 310 nm species? The extensive photochemical investigations of **1** and derivatives thereof have unambiguously shown that the chromophore responsible for this distinct and narrow absorption band is a dithioester group, that is, $-S-CH=S$.[35,36] The simplest radical of this configuration in our radical system would be the open-chain dithioester (TE) radical, $^\bullet CH_2SCH_2SCH=S$, $(1-TE)^\bullet$. As can easily be appreciated, this cannot be attained directly from $1^{\bullet+}$. But it could be generated via a simple ring opening (β-scission) of $1(-H)^\bullet$ (reaction 4), the radical formed upon proton loss of the radical cation. From the mechanistic point of view, $1^{\bullet+}$ is thus not the immediate precursor of the 310 nm species. Kinetically, reaction 3 is, however, the rate determining step for the formation of the 310 nm absorption; that is, $k_4 > k_3$. Radical $1(-H)^\bullet$, therefore, cannot be observed directly. Unambiguous evidence for it is, nevertheless, provided by experiments in the presence of oxygen, presented in the following.

In air-saturated solutions, of otherwise identical composition as in the N$_2$O-saturated systems, the 340 and 610 nm absorptions are not affected, either in yield (relative to available $^\bullet$OH yield) or in kinetics; that is, the underlying species do not react with oxygen under the experimental conditions. The 310 nm absorption, however, is almost completely quenched. Only upon a lowering of the oxygen concentration to less than 10^{-4} M, a small remainder of the dithioester-based absorption band is observed. (A complete series of experiments in the low oxygen concentration range could not be performed because of the lack of appropriate equipment for the exact determination of [O$_2$]. It turned out that by simply mixing air-saturated with N$_2$- or N$_2$O-saturated solutions gave results that showed too much scatter; that is, the uncertainties in oxygen concentration were too high.) These findings can only be explained by a competition between the ring opening of $1(-H)^\bullet$, yielding $(1-TE)^\bullet$ (reaction 4), and the oxygen addition to $1(-H)^\bullet$, yielding the cyclic peroxyl radical $1(-H)(OO^\bullet)$ (reaction 5). The latter lacks the dithioester chromophore and thus will not exhibit the characteristic 310 absorption band. Oxygen addition to the open chain $(1-TE)^\bullet$ radical, on the other hand, results in a peroxyl radical ($^\bullet OOCH_2SCH=S$) in which the chromophore remains intact; that is, the quenching of the 310 absorption can only be due to reaction 5 but not to reaction 6.

With $k_4 > k_3$, as stated above and the fact that in air-saturated solutions ([O$_2$] = 2×10^{-4} M) $k_5 \times$ [O$_2$] > k_4, this means that k_5 must be significantly above 10^8 M^{-1} s^{-1}. This is, indeed, to be expected in view of the usually diffusion controlled oxygen addition to most C-centered radicals (unless they carry strong electron density withdrawing substituents near the radical site which, however, is not the case here). Since the steady-state concentration of $1(-H)^\bullet$ is too low for direct detection of this radical, k_4 can reasonably be assumed to be at least 5–10 times faster than k_3 for the deprotonation of $1^{\bullet+}$, that is, be $(1-2) \times 10^5$ s^{-1}. This, in turn, would raise k_5 to $(0.5-1) \times 10^9$ M^{-1} s^{-1} (on the basis of $k_5 \times$ [O$_2$] = k_4). According to our experimental result, reaction 5 is, however, still much faster than reaction 4; that is, $k_5 \times$ [O$_2$] must even exceed $(1-2) \times 10^5$ s^{-1}. Allowing another factor of 5–10 for this pushes k_5 to about 10^{10} M^{-1} s^{-1}, which is pretty much the limit for a diffusion controlled oxygen addition. Taking the above-discussed lower and upper limits for $k_5 \times$ [O$_2$] into account, the most reasonable value for the ring opening reaction is considered to be $k_4 = 10^5$ s^{-1} ($\pm 30\%$), a value which is clearly within the range for such processes.

The decay of the 310 nm absorption occurs exponentially. An example representing the trace recorded from pH 10 solutions is displayed in Figure 2c. The rate constant derived from this and corresponding decay curves in the pH 9.0–10.4 range is $k_7 = (900 \pm 100)$ s^{-1}. At pH 4 a slightly lower value of 450 s^{-1} was obtained. In view of our assignment, the underlying process has to be the loss of the chromophore, that is, the destruction of the dithioester configuration. We consider this process to be hydrolysis as the relevant step for the destruction of the chromophore and as formulated specifically for the $(1-TE)^\bullet$ radical in reaction 7. (The monothio formic acid HOCH=S may, of course, further hydrolyze to formic acid).

$$^\bullet CH_2SCH_2SCH=S + H_2O \rightarrow {}^\bullet CH_2SCH_2SH + HOCH=S \tag{7}$$
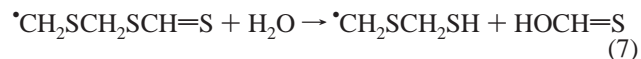
The same consideration concerning hydrolysis applies to any further product which carries a dithioester function. Prior to hydrolysis the $(1-TE)^\bullet$ radical may thus undergo β-scission (reaction 8), a process which may well occur on our experimental time-scale (but which will not be distinguishable through our detection means). The hydrolyzing species would then be the $^\bullet CH_2SCH=S$ radical.

$$^\bullet CH_2SCH_2SCH=S \rightarrow {}^\bullet CH_2SCH=S + CH_2=S \tag{8}$$

The hydrolyzing entity may, however, also be any nonradical species such as products from a radical–radical dimerization or disproportionation product, such as CH$_3$SCH$_2$SCH=S, CH$_3$-SCH=S, S=CHSCH$_2$SCH$_2$CH$_2$SCH$_2$SCH=S, S=CHSCH$_2$-SCH$_2$CH$_2$SCH=S, S=CHSCH$_2$CH$_2$SCH=S and others. Their bimolecular generation would not show up in the kinetics of the 310 nm decay since they all still carry the chromophore function. Most of them (in their methyl and phenyl substituted form) have, in fact, been identified and found to be subject to hydrolysis in photochemical studies of corresponding systems in acetonitrile solutions.[35,36,52] These considerations, by the way, nicely underpin our hypothesis that the decay of the 310 absorption solely results from the hydrolysis of the dithioester functionality and is not directly related to any reaction of the primary $(1-TE)^\bullet$ radical other than hydrolysis.

At this point we like to draw attention also to the conclusion derived below from the comparison between conductivity and
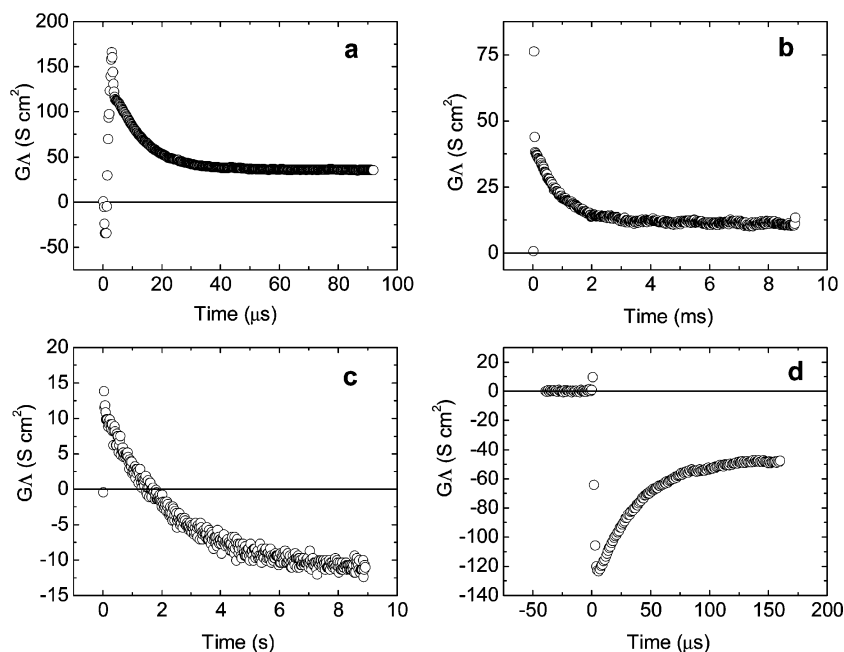
Figure 3. Conductivity-time traces obtained upon pulse radiolysis of pH 10, N_2O-saturated aqueous solutions of ca. 10^{-4} M **1** recorded in three different time domains: (a) microsecond time scale (the initial signal spikes, going into both directions, are equipment-inherent artifacts); (b) millisecond time scale; (c) time scale of seconds. Microsecond time scale trace at pH 4 is shown in panel d. Traces a, b, and c were collected in Bologna and trace d was collected at Notre Dame. The ordinate is shown in specific molar conductivity, in units of $S cm^2$.

optical data: that the 310 nm species is not the only product emerging from primary radical cation **1**[•+].

Pulse Radiolysis Conductivity Experiments. *pH 4.0−10.4 Solutions.* Complementary to the optical studies, experiments were carried out applying time-resolved conductivity as the detection method. Figure 3a−c shows conductivity-time traces recorded at pH 10.0 on three different time scales (the solutions were saturated with N_2O and **1**). Figure 3d shows an additional trace taken on the microsecond time scale at pH 4.

First of all, the conductivity signals provide direct proof of the formation and decay of a positively charged species, both at pH 10 and at pH 4.[6,46,53] Thus the initial signal increase of the conductivity in Figure 3a parallels that of the optical absorption in Figure 2a; that is, it is associable with the generation of **1**[•+]. The positive conductivity signal arises from the simultaneous formation of the radical cation (specific molar conductivity $\Lambda \approx 40-50$ S cm^{-1} at 18 °C) and the OH$^-$ ion ($\Lambda \approx 185$ S cm^{-1}) also inherently generated in reaction 2. The same conclusion is to be drawn from Figure 3d, that is, the experiment at pH 4. In the acidic solution, the OH$^-$ is, however, not stable as in the basic environment but will instantaneously react with a proton. Overall this leads to a displacement of a highly conducting H$^+$ ($\Lambda \approx 315$ S cm^{-1}) by the much less conducting **1**[•+]. The result, in this case, is a decrease in the conductivity signal. (For the interpretation of the conductivity traces (Figure 3a) it should be noted that the spikelike signals at very early times (≤ 1 μs) have no chemical meaning but are artifacts related to the electronics of the detection system.)

The conductivity data do not only provide kinetic data but also allow an estimation of the yields of the **1**[•+] radical cation. This has been done both on the basis of the signal increase in basic solution caused by the **1**[•+]/OH$^-$ ion pair ($\Lambda = 45 + 185 = 230$ S cm^{-1}) as well as of the decrease caused by the replacement of H$^+$ by **1**[•+] ($\Lambda = 45-315 = -270$ S cm^{-1}) in acid solution. The necessary reference was taken from thiocyanate and sulfoxide dosimetry systems, with •OH + 2 SCN$^-$ → OH$^-$ + (SCN)$_2$•$^-$ and •OH + (CH$_3$)$_2$SO → •CH$_3$ + CH$_3$SO$_2^-$ + H$^+$, respectively, as relevant processes. The result confirmed

that the yield of **1**[•+] is the same at pH 4 and in the pH 9.0−10.4 range (as found in the optical measurements) and corresponds to the yield of •OH radicals in N_2O-saturated solutions available for reaction with a 10^{-4} M solute; that is, G = 0.53 μmol J^{-1}. (In the analysis the signals have been extrapolated to their theoretical maximum by correction on the basis of their decay kinetics). This yield figure, in turn, was used for the estimation of the molar absorptivity of **1**[•+] at 610 nm and, in relation to that, of the other absorbing species (for actual values vide infra).

The decay of the conductivity signals, that is, decrease in basic solutions and increase in acid solutions after reaching the respective extremes, is indicative for a liberation of protons, for example, from **1**[•+] as formulated in reaction 3. In basic solution these protons will immediately be neutralized under consumption of OH$^-$ at a total yield equivalent to that of the originally present radical cations. In acid solutions the liberated protons simply restore the proton concentration which was lost in the radical cation formation process. If there was only one, and as such quantitative, proton liberation process, the signals would thus decay back to the original baseline irrespective of pH.

As can be realized from the time-resolved traces, especially in Figure 3a−c from the basic system, there are, however, at least three distinct steps in the decay of the initially generated signal. The largest occurs in the microsecond time domain covering about two-thirds of the initial signal (Figure 3a). The second apparent decay step takes place in the millisecond time range and amounts to about half of the remaining signal (or $^1/_6$ of initial maximum signal) (Figure 3b). On the time scale of seconds, finally, the rest of the positive signal decays and actually turns into a slightly negative signal (Figure 3c). The same features, although not specifically shown, apply also for the acid solution. In this case the signal eventually increases to above the original baseline at long times.

The first step in signal recovery kinetically coincides with the optical decay at 610 nm and is attributed to the deprotonation of **1**[•+]. The signal which still remains at the beginning of the

Transients in the Degradation of 1,3,5-Trithiane

J. Phys. Chem. A, Vol. 110, No. 29, 2006 **9297**

millisecond time domain can be explained by alternate and/or secondary processes. This suggestion is based on similar findings in the oxidation of simple thioethers as well as cyclic 1,3-dithia compounds. Contributing second-order processes, for example, could be the disproportionation of the radical cation itself and/or the C-centered α-thio radical generated in the deprotonation of $R_2S^{\bullet+}$.[6,8,54] Concerning the former, the redox disproportionation of two radical cations results in restored original sulfide and a dication, as formulated in reaction 9 in its general form. One dication contributes about the same conductivity as two original radical cations; that is, reaction 9 is not associated with any change in conductivity.

$$2(-S^{\bullet+}-) \rightarrow -S- + -S^{2+}- \qquad (9)$$
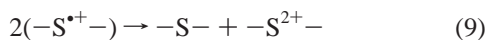
In aqueous environment the dication is a direct precursor of sulfoxide, a product positively identified in previous studies. In the simple thioether systems the presumed dication showed a lifetime well in the millisecond time domain. In our present systems the analogue reaction is clearly not a dominating process, but the small dose effect on the decay of $1^{\bullet+}$, mentioned above in the optical result section, is certainly indicative for some possible contribution to the longer lived conductivity.

Other cationic, longer-lived radical and molecular species may result from the disproportionation of $(1-TE)^{\bullet}$ (or its fragment radicals). Such type of reactions have been indicated in several related studies on the oxidation of simple thioethers and specifically also 1,3-dithia compounds.[6,34] To what extent any individual process (in part discussed in the literature and rationalized in the light of published work)[55-62] contributes to the conductivity changes in the millisecond time range cannot be decided on the basis of the accessible information in our present study. Because of this, we refrain from any detailed speculation on possibly underlying reactions. In any case, however, the decay of the conductivity signal in this time range (average $k_{II} = (1.5 \pm 0.5) \times 10^3$ s^{-1}) also refers to a liberation of protons from a cationic species.

The same, to some extent speculative nature has to be attested to possible reactions describing the third decay period on the time scale of seconds. One aspect, however, allows an unambiguous and important conclusion, and this is the eventual decay of the conductivity signal below the original baseline. This is indicative for a surplus of protons (relative to the original yield of primary radical cations) and a corresponding yield of anionic species. Although also somewhat speculative we want to offer at least one mechanistic rationale for this (eq 10), namely, the formation of formic acid and hydrogen sulfide, both generated upon hydrolysis of $HOCH=S$ (the latter being formed via reaction 7).

$$HOCH=S + H_2O \rightarrow HCO_2^- + 2\,H^+ + SH^- \qquad (10)$$

The formation of anion/proton pairs in such a process could even satisfactorily explain the signal change beyond the original baseline. In acid solution, where H^+ is stable, this causes a positive signal. In basic solution, on the other hand, the proton consumes an OH^-. The overall result is then a replacement of the highly conducting hydroxyl ion by a normal anion, that is, a loss of conductivity. Kinetically, the third change in conductivity is described by an exponential curve with a first-order rate constant of $k_{III} \approx (0.5 \pm 0.2)$ s^{-1} (pH 9.0-10.4).

Considering the variety of products possibly formed in the oxidation of **1,** it is certainly not justified to assign absolute yields to any contributor to the conductivity except the primary $1^{\bullet+}$ radical cation. It should also be mentioned that the kinetics
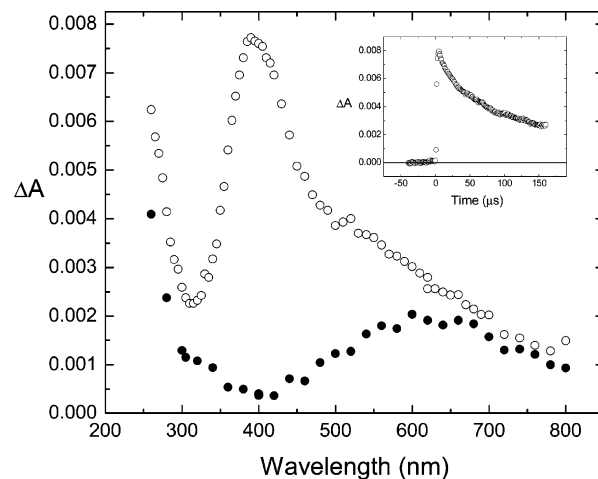
Figure 4. Transient absorption spectra recorded after radiolysis of **1** in N$_2$O-saturated (open circles) and O$_2$-saturated (filled circles) solutions, pH 1 ([**1**] ca. 10^{-4} M). Inset shows the kinetic trace at 400 nm, N$_2$O-saturated solution.

explicitly evaluated refer to the main directly observable processes. In several cases the, in our mind most reasonable, results obtained on the basis of a monoexponential could still be further adjusted to bi- or tri- exponentials. We do not see any justification though for any additional mechanistic speculation in this direction. Irrespective of these considerations, the overall conductivity results tie well into that mechanism outlined and discussed above.

Acid Solutions (pH 1). Experiments conducted with very acidic solutions revealed some further and new aspects. An expected finding upon pulse radiolysis of N$_2$O-saturated solutions of **1** is a smaller initial yield for the absorption of $1^{\bullet+}$ as compared with pH ≥ 4. This is simply due to a smaller concentration of $^{\bullet}OH$ radicals owing to the competition between N$_2$O and H$^+$ for the hydrated electrons. At low enough pH (e.g., at pH 1) eventually all hydrated electrons are converted into hydrogen atoms.

$$e_{aq}^- + H^+ \rightarrow H^{\bullet} \qquad (11)$$

Under these conditions, the yields of H$^{\bullet}$ (G ≈ 0.33 μmol J^{-1}) and $^{\bullet}OH$ (G ≈ 0.28 μmol J^{-1}) are almost equal. Although halved in yield as compared to the N$_2$O-saturated solution at pH ≥ 4, the formation kinetics of $1^{\bullet+}$ by the remaining primary $^{\bullet}OH$ and its subsequent conversion into the long-lived 310 nm dithioester radical remained unaffected.

A completely new finding is, however, the fast formation of a strong and relatively broad absorption band with λ_{max} at 400 nm. Its formation is completed within the first 1-2 μs, that is, occurs with a rate constant of about 10^{10} M^{-1} s^{-1} assuming the direct involvement of **1**. The lifetime of the 400 nm species differs significantly from that of all the other species presented and discussed above. Under our experimental conditions it decays with a first half-life of about 70 μs in a process which appears to involve more than just one exponential (see inset to Figure 4).

In the presence of oxygen the 400 nm absorption is completely suppressed while the 610 nm band of the $1^{\bullet+}$ radical cation is not affected. For comparison, the transient spectra recorded at about 3 μs after the pulse in N$_2$O and O$_2$-saturated solutions, respectively, are shown in Figure 4. This is a most informative result because it strongly hints at the H$^{\bullet}$ atom to be responsible for the formation of the 400 nm species because of the efficient scavenging of hydrogen atoms by oxygen (H$^{\bullet}$ +

SCHEME 2

**CHART 2**

| 370 nm | 400 nm | 440 nm | 465 nm |
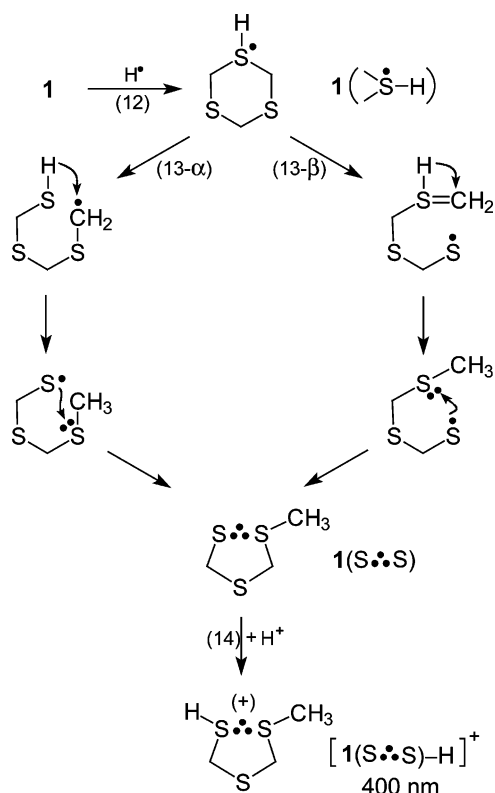
$O_2 \rightarrow HO_2{}^{\bullet}$). On the basis of this observation and the fast, that is, diffusion-controlled formation kinetics, we postulate the mechanism outlined in Scheme 2 with a cyclic, three-electron bonded radical cation as the absorbing transient.

The first step (reaction 12) is considered to be an addition of the hydrogen atom to one of the sulfur atoms in **1** to yield the still cyclic sulfuranyl-type **1**($>S^{\bullet}-H$) radical. We exclude the alternative possibility of an H abstraction from one of the CH_2 groups for two reasons. (i) Such a process should be associated with some activation energy, that is, occur with a much slower rate constants than observed; and (ii) an H abstraction would lead to the C-centered radical **1**$(-H)^{\bullet}$ which in the absence of oxygen exclusively results in the formation of the dithioester radical $(\mathbf{1}-TE)^{\bullet}$. The $(\mathbf{1}-TE)^{\bullet}$ (310 nm)/$\mathbf{1}^{\bullet+}$ (610 nm) yield ratio remains, however, the same (≈ 2) as in neutral and basic solution while it should assume double that figure if $(\mathbf{1}-TE)^{\bullet}$ was also formed via $H^{\bullet}$ reaction.

The next step is considered to be the ring opening of **1**($>S^{\bullet}-H$). Two possibilities can be envisaged, α-scission and β-scission (Scheme 2, reaction 13-α and 13-β). Both lead to the same result, namely, intermediate open-chain thiyl radicals which by intramolecular coupling with the free electron pair of a second sulfur form the cyclic $2\sigma/1\sigma^*$ three-electron bonded neutral radical **1**($S\therefore S$). Both pathways involve well established and straightforward follow-up steps. We give preference to the β-scission because this is the more common process in radical chemistry.

Neutral species of the type **1**($S\therefore S$) structure are not very stable and usually equilibrate toward the separate $-S^{\bullet}$ and $:S-$ entities. Proton attachment to **1**($S\therefore S$) (reaction 14), however, further stabilizes the structure through the possibility of charge delocalization. The $[\mathbf{1}(S\therefore S)-H]^+$ radical cation thus formed is assumed to be the species responsible for the 400 nm band. A desirable confirmation of the cationic property through time-resolved conductivity is, unfortunately, not possible because
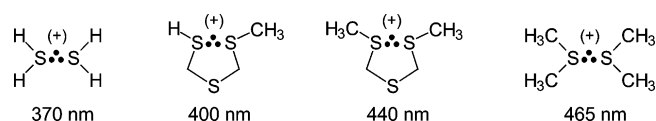
such measurements cannot be performed in solutions of high ion concentration as it prevails at pH < 3.[46] The optical properties of $[\mathbf{1}(S\therefore S)-H]^+$ corroborate well with those of similar three-electron bonded species. As mentioned before, the position of λ_{max} sensitively depends on two parameters, structure and substitution.[1-4,6-9,12,13] Any structure which supports a favorable p orbital overlap of the two interacting sulfur atoms (such as five-membered rings) results in a more blue-shifted absorption (besides enhancing the thermodynamic stability of the $S\therefore S$ bond). Electron density releasing substituents at the sulfur atoms, on the other hand, typically yield increasingly red-shifted absorptions (besides weakening the $S\therefore S$ bond). Considering these parameters, our presumed $[\mathbf{1}(S\therefore S)-H]^+$ radical cation ties very well into a series of other well-established $S\therefore S$ bonded radical cations.[1-4,6-13,28,63] For comparison the structures and the respective λ_{max} of three examples are shown together with $[\mathbf{1}(S\therefore S)-H]^+$ in Chart 2. The effect of electron density release from CH_3 versus H becomes particularly apparent in the red shift from 370 to 465 nm for the fully H- and CH_3-substituted noncyclic $(>S\therefore S<)^+$, respectively. The same trend results from substitution of just one methyl group by hydrogen as shown in the comparison between our present $[\mathbf{1}(S\therefore S)-H]^+$ species with the 440 nm radical cation of the same cyclic structure which carries a methyl group instead of a hydrogen. (The third, remote sulfur in $[\mathbf{1}(S\therefore S)-H]^+$ has little effect and if so would induce a rather small red shift). A structure-based stabilization is indicated by the blue shift from 465 to 440 nm for the open vs cyclic radical cation despite the all-alkyl substitution at the two sulfur atoms. In conclusion, our assignment of the 400 nm absorption to $[\mathbf{1}(S\therefore S)-H]^+$ finds full support in light of the well-known optical properties of $2\sigma/1\sigma^*$ three-electron bonded radical species.

Coming back to our experiments at pH 4 and in basic solutions it seems not unreasonable to assign the small absorption around 400 nm observed in these systems (see, for example Figure 1) also to an $(S\therefore S)$-bonded species. Although fully alkylated species of this kind have been found[6] to be long-lived enough for observation on the microsecond time scale up to pH 10, we cannot exclude, however, that $[\mathbf{1}(S\therefore S)-H]^+$ may already be deprotonated and possibly even be converted into a completely different follow-up species. This ambiguity is also a reflection of the relatively low yield of the initiating H atoms in this pH range and the relatively small absorption around 400 nm. All this precludes any speculation on the actual identity the species under discussion.

Molar Absorption Coefficients of Absorbing Transients. As pointed out above, the conductivity experiments allowed an evaluation of the molar absorption coefficient of the $\mathbf{1}^{\bullet+}$ radical cation. The obtained value of $\epsilon(\mathbf{1}^{\bullet+})_{610} = 775$ M^{-1} cm^{-1} is in agreement with an earlier determined one of 723.[30] An estimation of the same molar absorption coefficient on the basis of the results from pulse radiolysis with optical detection (Figure 1a) leads to the value of (1000 ± 150) M^{-1} cm^{-1}. Owing to the inherent distortion of the conductivity signals at early (<1 μs) times, the optically derived value is considered to be the more accurate one and thus used for correlation with other molar extinction coefficients.

Assuming a quantitative conversion of $\mathbf{1}^{\bullet+}$ into $(\mathbf{1}-TE)^{\bullet}$ and the observation that the optical absorption of this latter radical

Transients in the Degradation of 1,3,5-Trithiane

J. Phys. Chem. A, Vol. 110, No. 29, 2006 **9299**

at 310 nm is 2.25 times higher than that of the radical cation at 610 nm (see Figure 1) would yield a molar absorption coefficient for the dithioester radical of $\epsilon(\mathbf{1}{-}\text{TE})^\bullet_{310} \approx 2250$ M^{-1} cm^{-1}. This is about 4 to 5 times lower than the value ($\approx 1 \times 10^4$ M^{-1} cm^{-1}) reported for molecular dithioester products in photochemical studies on methylated derivatives of **1** in acetonitrile solutions.[35] Although the respective ϵ values must by no means be identical, we see no plausible reason for such a large difference. It is much more likely that the yield of $(\mathbf{1}{-}\text{TE})^\bullet$ is considerably lower than the yield of its reference $(\mathbf{1}^{\bullet+})$ precursor. In fact, this conclusion was corroborated by our conductivity data in the millisecond time range which suggested the likelihood of alternate decay routes of $\mathbf{1}^{\bullet+}$ besides simple deprotonation. Any further identification and quantification of these latter processes are beyond the scope of this study. Nevertheless, we conclude that the molar absorption coefficient of the $(\mathbf{1}{-}\text{TE})^\bullet$ radical is significantly higher than the above evaluated figure and close to the photochemically determined value for molecular dithioester compounds.

The $[\mathbf{1}(S\therefore S){-}H]^+$ radical cation shows, by comparison, a four times higher absorption at 400 nm than $\mathbf{1}^{\bullet+}$ at 610 nm (see Figure 4). Taking into account that the yield of H$^\bullet$ atoms, which are responsible for the formation of $[\mathbf{1}(S\therefore S){-}H]^+$, is probably about 15% higher in pH 1 solutions than the available $^\bullet$OH yield for the generation of $\mathbf{1}^{\bullet+}$, leads to a molar absorption coefficient for the three-electron bonded radical cation of $\epsilon[\mathbf{1}(S\therefore S){-}H]^+_{400} = (4700 \pm 500)$ M^{-1} cm^{-1}. This fits very well into the range of molar absorptivities determined for other $2\sigma/1\sigma^*$ radical ions.

Conclusion

Radical chemistry studies on 1,3,5-trithiane (**1**), performed by radiation chemical means, have provided further insight into the one-electron oxidation of this compound and the role of sulfur as a potential target of H atom attack. Several transients, rate constants, and mechanistic details could be identified, measured, and revealed. Comparison of our present results with earlier photochemical investigations underpin the valuable complementarity of photochemistry and radiation chemistry. At the same time, differences are clearly apparent. They pertain in particular to the formation of radical cations and other ionic species in the radiation chemical systems.

References and Notes

(1) Asmus, K.-D. *Acc. Chem. Res.* **1979**, *12*, 436.
(2) Asmus, K.-D. In *Sulfur-Centered Reactive Intermediates in Chemistry and Biology;* Chatgilialoglu, C., Asmus, K.-D., Eds.; NATO-ASI Series A, Life Sciences; Plenum Press: New York, 1990; Vol. 197, p 155.
(3) Asmus, K.-D.; Bonifacic, M. In *S−Centered Radicals;* Alfassi, Z. B., Ed.; John Wiley & Sons Ltd.: Chichester, U.K., 1999; p 141.
(4) Asmus, K.-D. In *Radiation Chemistry: Present Status and Future Prospects;* Jonah, C. D., Rao, B. M. S., Eds.; Elsevier: Amsterdam, The Netherlands, 2001; Vol. 87, p 341.
(5) Asmus, K.-D. *Nukleonika* **2000**, *45*, 3.
(6) Bonifacic, M.; Möckel, H.; Bahnemann, D.; Asmus, K.-D. *J. Chem. Soc., Perkin Trans. 2* **1975**, 675.
(7) Asmus, K.-D.; Bahnemann, D.; Fischer, C.-H.; Veltwisch, D. *J. Am. Chem. Soc.* **1979**, *101*, 5322.

(8) Mönig, J.; Goslich, R.; Asmus, K.-D. *Ber. Bunsen-Ges. Phys. Chem.* **1986**, *90*, 115.
(9) Göbl, M.; Bonifacic, M.; Asmus, K.-D. *J. Am. Chem. Soc.* **1984**, *106*, 5984.
(10) Clark, T. *J. Comput. Chem.* **1981**, *2*, 261.
(11) Clark, T. *J. Am. Chem. Soc.* **1988**, *110*, 1672.
(12) Gill, P. M. W.; Radom, L. *J. Am. Chem. Soc.* **1988**, *110*, 4931.
(13) Illies, A. J.; Livant, P.; McKee, M. L. *J. Am. Chem. Soc.* **1988**, *110*, 7980.
(14) Bonifacic, M.; Asmus, K.-D. *J. Chem. Soc., Perkin Trans. 2* **1980**, 758.
(15) Anklam, E.; Mohan, H.; Asmus, K.-D. *J. Chem. Soc. Chem. Commun.* **1987**, 629.
(16) Hungerbühler, H.; Guha, S. N.; Asmus, K.-D. *J. Chem. Soc. Chem. Commun.* **1991**, 999.
(17) Tobien, T.; Hungerbühler, H.; Asmus, K.-D. *Phosphorus, Sulfur Silicon Relat. Elem.* **1994**, *95/96*, 249.
(18) Asmus, K.-D.; Göbl, M.; Hiller, K.-O.; Mahling, S.; Mönig, J. *J. Chem. Soc., Perkin Trans. 2* **1985**, 641.
(19) Glass, R. S.; Hojjatie, M.; Wilson, G. S.; Mahling, S.; Göbl, M.; Asmus, K.-D. *J. Am. Chem.* Soc. **1984**, *106*, 5382.
(20) Glass, R. S.; Hojjatie, M.; Petsom, A.; Wilson, G. S.; Göbl, M.; Mahling, S.; Asmus, K.-D. *Phosphorus Sulfur Relat Elem.* **1985**, *23*, 143.
(21) Alder, R. W.; Bonifacic, M.; Asmus, K.-D. *J. Chem. Soc., Perkin Trans. 2* **1986**, 277.
(22) Mahling, S.; Asmus, K.-D.; Hojjatie, M.; Glass, R. S.; Wilson, G. S. *J. Org. Chem.* **1987**, *52*, 3717.
(23) Bobrowski, K.; Hug, G. L.; Marciniak, B.; Miller, B. L.; Schöneich, C. *J. Am. Chem. Soc.* **1997**, *119*, 8000.
(24) Bobrowski, K.; Pogocki, D.; Schöneich, C. *J. Phys. Chem. A* **1998**, *102*, 10512.
(25) Chaudhri, S. A.; Asmus, K.-D. *Angew. Chem. (Deutsche Ausgabe)* **1981**, *91*, 690.
(26) Chaudhri, S. A.; Asmus, K.-D. *Angew. Chem., Int. Ed. Engl.* **1981**, *20*, 672.
(27) Chaudhri, S. A.; Gobl, M.; Freyholdt, T.; Asmus, K.-D. *J. Am. Chem. Soc.* **1984**, *106*, 5988.
(28) Chaudhri, S. A.; Mohan, H.; Anklam, E.; Asmus, K.-D. *J. Chem. Soc., Perkin Trans. 2* **1996**, 383.
(29) Bahnemann, D.; Asmus, K.-D. *J. Chem. Soc. Chem. Commun.* **1975**, 238.
(30) Asmus, K.-D.; Bahnemann, D.; Bonifacic, M.; Gillis, H. A. *Faraday Discuss. Chem. Soc.* **1978**, *63*, 213.
(31) Bock, H.; Wagner, G. *Angew. Chem.* **1972**, *84*, 119.
(32) Potzinger, P. Private communication.
(33) Asmus, K.-D.; Gillis, H. A.; Teather, G. G. *J. Phys. Chem.* **1978**, *82*, 2677.
(34) Bonifacic, M.; Asmus, K.-D. *J. Org. Chem.* **1986**, *51*, 1216.
(35) Janeba-Bartoszewicz, E.; Hug, G. L.; Kozubek, H.; Urjasz, W.; Marciniak, B. *J. Photochem. Photobiol., A* **2001**, *140*, 133.
(36) Janeba-Bartoszewicz, E.; Hug, G. L.; Andrzejewska, E.; Marciniak, B. *J. Photochem. Photobiol., A* **2006**, *177*, 17.
(37) Holmes, B. E.; Navon, G.; Stein, G. *Nature* **1967**, *213*, 1087.
(38) Ferreri, C.; Costantino, C.; Landi, L.; Mulazzani, Q. G.; Chatgilialoglu, C. *Chem. Commun.* **1999**, 407.
(39) Wisniowski, P.; Bobrowski, K.; Carmichael, I.; Hug, G. L. *J. Am. Chem. Soc.* **2004**, *126*, 14468.
(40) Wisniowski, P.; Bobrowski, K.; Filipiak, P.; Carmichael, I.; Hug, G. L. *Res. Chem. Intermed.* **2005**, *31*, 633.
(41) Janata, E.; Lilie, J.; Martin, M. *Radiat. Phys. Chem.* **1994**, *43*, 353.
(42) Hug, G. L.; Wang, Y.; Schöneich, C.; Jiang, P.-Y.; Fessenden, R. W. *Radiat. Phys. Chem.* **1999**, *54*, 559.
(43) Mirkowski, J.; Wisniowski, P.; Bobrowski, K. *INCT Annual Report*; Warsaw, Poland, 2000; p 31.
(44) Bobrowski, K. *Nukleonika* **2005**, *50* (Suppl, 3), S67.
(45) Asmus, K.-D. In *Oxygen Radicals in Biological Systems*; Packer, L., Ed.; Academic: Orlando, FL, 1984; Vol. 105, p 167.
(46) Asmus, K.-D.; Janata, E. In *The Study of Fast Processes and Transient Species by Electron Pulse Radiolysis*; Baxendale, J. H., Busi, F., Eds.; D. Reidel Publ. Co.: Dordrecht, Holland, 1982; p 91.
(47) Veltwisch, D.; Janata, E.; Asmus, K.-D. *J. Chem. Soc., Perkin Trans. 2* **1980**, 146.
(48) Janata, E. *Radiat. Phys. Chem.* **1982**, *19*, 17.
(49) Bobrowski, K.; Schöneich, C. *J. Chem. Soc., Chem. Commun.* **1993**, 795.
(50) Schöneich, C.; Bobrowski, K. *J. Am. Chem. Soc.* **1993**, *115*, 6538.
(51) Meissner, G.; Henglein, A.; Beck, G. *Z. Naturforsch., B: Chem. Sci.* **1967**, *22*, 13.
(52) Janeba-Bartoszewicz, E.; Marciniak, B. Unpublished results.
(53) Asmus, K.-D. In *Fast Processes in Radiation Chemistry and Biology*; Adams, G. E., Fielden, E. M., Michael, B. D., Eds.; Wiley: New York, 1975; p 40.
(54) Hiller, K.-O.; Asmus, K.-D. *J. Phys. Chem.* **1983**, *87*, 3682.

(55) Russell, G. A.; Law, W. C. In *Sulfur-Centered Reactive Intermediates in Chemistry and Biology,* Chatgilialoglu, C., Asmus, K.-D., Eds.; NATO-ASI Series A, Life Sciences; Plenum Press: New York, 1990; Vol. 197, p 173.

(56) Russell, G. A.; Law, W. C.; Zaleta, M. *J. Am. Chem. Soc.* **1985**, *107*, 4175.

(57) Russell, G. A.; Underwood, G. R.; Lini, D. C. *J. Am. Chem. Soc.* **1967**, *89*, 6636.

(58) Hug, G. L.; Janeba-Bartoszewicz, E.; Filipiak, P.; Kozubek, H.; Marciniak, B. In preparation.

(59) Eigen, M. *Angew. Chem.* **1963**, *75*, 486.

(60) Eigen, M.; De Maeyer, L. In *Technique of Organic Chemistry*, 2nd ed.; Weissberger, A., Ed.; Interscience: New York, 1961; Vol. VIII.

(61) Eigen, M.; Kruse, W.; Maass, G.; De Maeyer, L. In *Progress in Reaction Kinetics*; Porter, G., Ed.; Pergamon: Oxford, NY, 1964; Vol. II, p 285.

(62) Chaudhri, S. A.; Asmus, K.-D. *J. Chem. Soc., Faraday Trans. 1* **1972**, *68*, 385.

(63) Deng, Y.; Illies, A. J.; McKee, M. L.; Peschke, M. *J. Am. Chem. Soc.* **1995**, *117*, 420.